Synthesis and Performance Study of Photodetectors of Low-Dimensional Perovskites

Hongxiang Ding *

Dalian Maritime University, Dalian 116000, China

* Corresponding Author Email: Dmudhx@163.com

Abstract. This paper reviews the recent advancements in perovskite-structured photodetectors, highlighting the significance of their dimensional variations, which range from 0D quantum dots to 1D nanowires and microwires, and further to 2D nanostructures. It examines the various synthesis and modification techniques used to optimize these structures, along with their compositional variations. Additionally, the paper assesses the photodetection performance of these devices and explores their potential applications. Furthermore, a comprehensive summary of the key quality factors for photodetectors, the unique photoelectric properties of low-dimensional perovskites, and the methods for their synthesis is provided, offering a comprehensive overview of the current research landscape in this field.

Keywords: Low-Dimensional Perovskites, Photodetectors, Photoelectric Properties, Synthesis Methods.

1. Research Background

Photodetectors, devices capable of converting optical signals into electrical signals, are widely used in imaging, communication, biomedical, and security applications. The performance of photodetectors primarily depends on the photoelectric characteristics of the semiconductor materials used, such as the light absorption coefficient, carrier mobility, carrier lifetime. Traditional semiconductor materials, like silicon, cadmium telluride, and mercury cadmium telluride, though high in photoelectric conversion efficiency, have drawbacks like high cost, complex fabrication processes, fixed band gaps, low sensitivity. Therefore, finding new semiconductor materials to enhance the performance and keep costs as low as possible is a current research focus and challenge.

In recent years, organic-inorganic hybrid halide perovskites (simply referred to as perovskites) have emerged as a new type of semiconductor material, attracting widespread attention and research. Perovskites, characterized by low defect density and shallow energy traps, effectively reduce carrier recombination, enhancing carrier mobility, thereby exhibiting excellent charge transport properties [1] [3]. Additionally, perovskites can be prepared through a simple solution process under low temperatures without the need for complex and expensive vacuum equipment, reducing production costs and complexity [1] [4]. Importantly, perovskites can form various dimensional nanostructures, such as 0D, 1D, 2D, and 3D, which can modulate the band structure, carrier transport, and optical properties of perovskites, optimizing the performance of photodetectors [1]. Based on these advantages, halide perovskites have recently become promising candidates for next-generation photodetectors. However, traditional three-dimensional halide perovskite photodetectors inevitably suffer from defects and grain boundaries, leading to issues like current-voltage hysteresis, unreliable performance, and instability. Low-dimensional halide perovskites, due to their unique electrical and optical properties, demonstrate enhanced reliability and stability in ultrafast photo response, broad detection bands, and ultra-sensitive detection. Significant research and innovation have been conducted to overcome these issues.

This paper reviews the significant research and progress in low-dimensional perovskite photodetectors, elaborating in detail beforehand on the quality factors related to photodetectors, the main optical properties of low-dimensional perovskites, and introduces the current popular synthesis methods for low-dimensional perovskite materials. Finally, it discusses the limitations of low-

dimensional perovskites in the field of photodetectors, comments on potential solutions to these challenges, and provides an inspiring outlook on their future development direction.

2. Synthesis of Low-Dimensional Perovskites

In recent years, as research into the properties of low-dimensional perovskite photodetectors has deepened, a variety of synthesis methods, including solution processing, vapor deposition, and templating techniques, have been explored by researchers. Different synthesis methods directly affect the performance characteristics of photodetectors, thus mastering various synthesis techniques and selectively employing them based on requirements is crucial in exploring perovskite photodetectors. [17]

2.1. Solution Synthesis

Solution synthesis is a common method for fabricating low-dimensional perovskite materials. It allows for the control of morphology, composition, and structure of perovskites, thereby influencing their photoelectric properties. Main methods of solution synthesis include hot-injection, self-assembly, ion-exchange, and hydrothermal methods. These methods can produce various dimensional perovskite nanostructures like quantum dots, nanowires, nanosheets, as well as heterostructures and flexible photodetectors based on low-dimensional perovskites.

The solution synthesis of low-dimensional perovskite materials generally involves the following steps:

(i) Select appropriate organic and inorganic cations, such as methylammonium (MA), phenylethyl ammonium (PEA), lead (Pb), tin (Sn), iodine (I), and bromine (Br), and mix them in a certain molar ratio in organic solvents like dimethylformamide (DMF) or dimethyl sulfoxide (DMSO) to prepare a perovskite precursor solution.

(ii) Deposit the perovskite precursor solution onto a suitable substrate, like glass, silicon, or oxides, by spin-coating or drop-casting to form a uniform film.

(iii) Anneal the film on a temperature-controlled hotplate or in an oven to crystallize the perovskite precursor, forming low-dimensional perovskite crystals.

Deng and others used a simple solution scraping method to prepare one-dimensional oriented single-crystal $CH_3NH_3PbI_3$ MW arrays. [18] As shown in Figure 1a, a blade drags the $CH_3NH_3PbI_3$ solution in dimethylformamide across a substrate heated at 100°C, forming highly oriented $CH_3NH_3PbI_3$ MW arrays with lengths up to several centimeters, while simultaneously the substrate changes color from yellow to black. As shown in Figures 1b and c, the $CH_3NH_3PbI_3$ MW primarily aligns along the direction of the blade's movement.

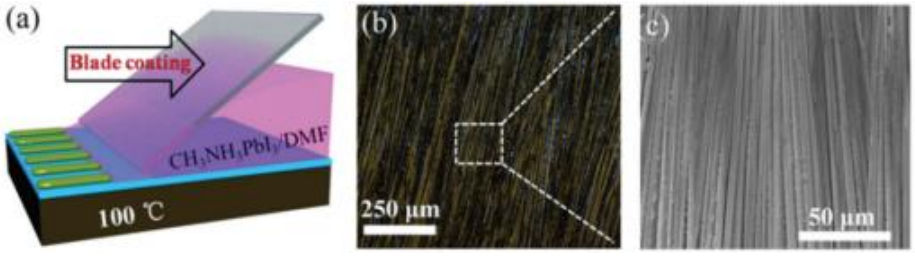

Figure 1. a) Schematic illustration of the one-step blade coating process for the fabrication of single-crystalline CH3NH3PbI3 MW arrays. b) Optical microscope and c) SEM images of the MW arrays fabricated with a blade coating speed of 60 μm s^{-1} at 100°C.

2.2. Vapor Deposition

Vapor deposition is a high-temperature, high-vacuum method, which can be categorized into chemical vapor deposition (CVD), atomic layer deposition (ALD), and physical vapor deposition (PVD). The advantage of this method is the production of high-quality, high-purity, highly crystalline, and low-defect low-dimensional perovskite materials with precise control over thickness, morphology,

composition, and structure. However, it requires expensive equipment, complex process parameters, strict environmental conditions, and challenges in achieving large-area, uniform, and continuous low-dimensional perovskite thin films. Below, we introduce the chemical vapor deposition (CVD) and physical vapor deposition (PVD) methods.

2.2.1. Chemical Vapor Deposition (CVD)

CVD is a method where gaseous reactants undergo chemical reactions on a solid substrate to form thin films. It can produce high-quality, high-purity, highly crystalline, and low-defect perovskite materials with precise control over thickness, morphology, composition, and structure. The general steps for preparing perovskite photodetectors using CVD are as follows:

(i) Place the substrate (like glass, silicon, or oxides) inside a heated quartz tube in a vacuum chamber and preheat to a certain temperature (e.g., 30℃).

(ii) Place a mixture of organic cations (like methylammonium, phenylethyl ammonium) and metal halides (like lead iodide, lead bromide) in another heated quartz tube and heat to a certain temperature (e.g., 15℃) to vaporize them into a gaseous state.

(iii) Transport the gaseous reactants to the quartz tube containing the substrate using an inert gas (like nitrogen, argon), causing a chemical reaction on the substrate to form a perovskite thin film.

(iv) Adjust reaction time, temperature, pressure, and gas flow to control the thickness, morphology, composition, and structure of the perovskite film.

(v) Deposit appropriate electrode materials (like gold, silver, indium tin oxide) on the perovskite film to form the structure of the photodetector.

Deng and others successfully prepared $CH_3NH_3SnI_3$ perovskite nanowires using chemical vapor deposition. [19] SnI was used as a single source, placed in a quartz tube mounted on a single-zone tube furnace at 18℃. Freshly cut mica substrates were pre-cleaned with anhydrous ethanol and placed in the downstream area of the quartz tube. First, the quartz tube was vacuumed to −0.09 MPa, and a certain amount of high-purity hydrogen (H_2) was introduced to prepare the precursor. The temperature and pressure inside the quartz tube were set and stabilized at 395℃, 0 MPa, and after a certain deposition time, SnI_2 nanosheets were formed, allowing the tube furnace to cool naturally to room temperature. Then, the SnI2 precursor and methylammonium iodide (CH_3NH_3I) were placed in a clean quartz tube. The SnI_2 nanosheets on the mica were placed in the downstream area, while CH_3NH_3I was placed in the center of the quartz tube. Under 125℃, 0.0026 MPa, and a high-purity argon (Ar) atmosphere, after a certain reaction time, SnI_2 was successfully converted to $CH_3NH_3SnI_3$ perovskite.

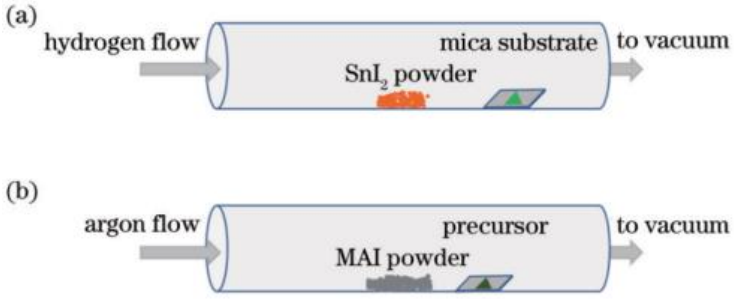

Figure 2. Two-step vapor deposition method experimental setup diagram. a) Schematic of the synthesis setup for SnI_2 nanosheets; b) Schematic of the setup for the synthesis of $CH_3NH_3SnI_3$ nanosheets.

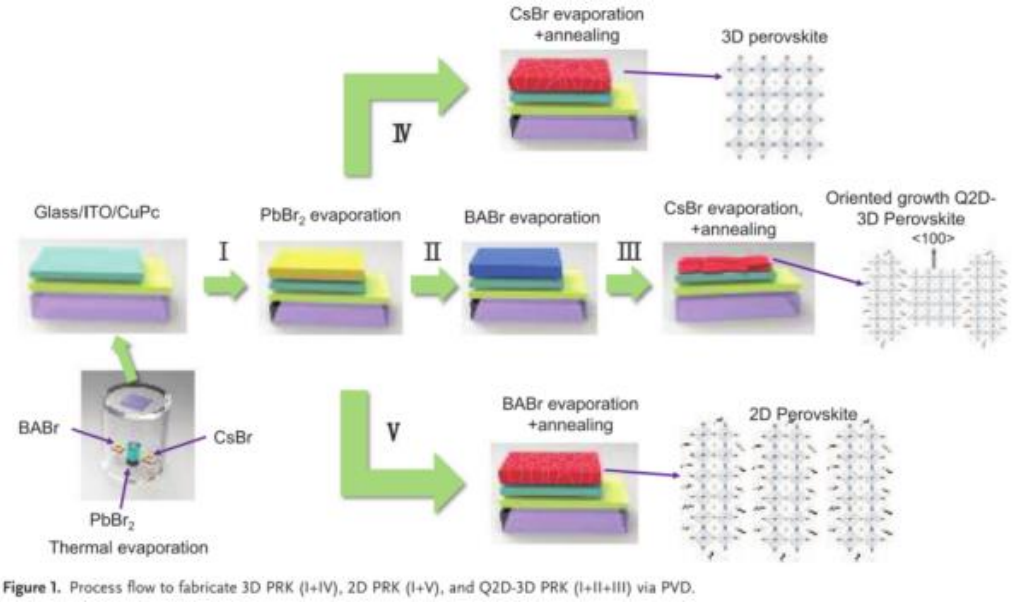

Figure 1. Process flow to fabricate 3D PRK (I+IV), 2D PRK (I+V), and Q2D-3D PRK (I+II+III) via PVD.

Figure 3. Process flow to fabricate 3D PRK (I+IV), 2D PRK (I+V), and Q2D-3D PRK (I+II+III) via PVD.

2.3. Template Method

The template method is a technique that employs externally added or self-assembled templates to control the morphology and structure of materials, which can be used for the preparation of low-dimensional perovskites. The advantage of the template method is that it can produce highly ordered and adjustable micro/nanostructures, thereby improving the performance and stability of photodetectors. The disadvantages include the need for additional template materials, steps for removing the templates, which may increase cost and complexity, and potential damage or contamination of the perovskite materials. Below, we introduce two types of template methods: hard template method and soft template method.

2.3.1. Hard Template Method

The hard template method involves using rigid solid materials as templates, depositing or filling perovskite materials onto the templates by physical or chemical methods, and then removing the templates to achieve the desired morphology and structure. This method can produce a variety of morphologies for low-dimensional perovskite photodetectors, such as nanowires, nanotubes, nanorods, and nanopores. The advantages of the hard template method include the ability to create high-precision, uniform, and complex micro/nanostructures, and precise control over the composition and structure of the perovskite materials. The downsides are the requirements for high temperatures, high vacuum, or etching conditions, which may affect the quality and stability of the perovskite materials, as well as difficulties in achieving large-area, continuous micro/nanostructures.

Hu and colleagues used large-scale roll-to-roll microgravure printing and doctor blading to fabricate large-area nanowire arrays, a typical example of the hard template method. [21] They first deposited the perovskite precursor solution onto PET or SiO_2 substrates, and then formed a perovskite film by doctor blading. Perovskite nanowires gradually formed within the perovskite film prepared by doctor blading and were then treated in an oven for 10 minutes to accelerate the complete formation of the CH3NH3PbI3 perovskite nanowire structure, as shown in Figure 4.

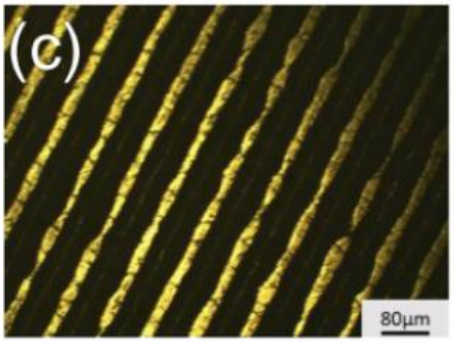

Figure 4. $CH_3NH_3PbI_3$ perovskite nanowire structure fabricated using the hard template method.

2.3.2. Soft Template Method

The soft template method involves using flexible liquid or solid materials as templates, forming perovskite materials within these templates through self-assembly or phase separation methods, and then removing the templates to obtain the desired morphology and structure. This method can produce various morphologies for low-dimensional perovskite photodetectors, such as nanoplates, nanospheres, nanoflowers, and nanonets. The advantages of the soft template method are the ability to create low-temperature, low-cost, simple micro/nanostructures, and the adjustable control over the morphology and size of the perovskite materials. However, the soft template method has disadvantages in achieving high-precision, uniformity, and complexity in the micro/nanostructures, and in the precise control of the composition and structure of the perovskite materials.

Li and colleagues synthesized $MAPbBr_3$ single-crystal microwire arrays (SCMWAs) using the soft template method. [22] Initially, a PDMS template with a periodic microgroove-protrusion structure was tightly attached to a substrate to form a series of sealed periodic microchannels. To prevent the PDMS template from being blown away by the solvent evaporating from the substrate, a spacer was used at one end of the template to create an opening for the solvent vapor to escape from the microchannels, as shown in Figure 1. As shown in Figure 5a, under the influence of capillary forces, the MAPbBr3 precursor quickly flowed into these periodic microchannels after being deposited at one end of the template, as illustrated in Figures 5b and 5c. Upon appropriate heating at about 6°C, the solvent gradually evaporated. Due to the sealed microchannels, the solvent evaporation process was confined within the microchannels, and the liquid could only flow along the direction of the microchannels. Moreover, as the liquid flowed through the channels, two liquid tails attached to each side wall of the microchannels formed a moving three-phase contact line along the side walls, as shown in Figure 5d. These tails led to preferential crystallization along the sidewalls, producing high-quality $MAPbBr_3$SCMWAs, as depicted in Figure 5e. After the solvent evaporation process was completed, the PDMS template and spacer were peeled off from the substrate, leaving highly aligned $MAPbBr_3$SCMWA on the substrate, as shown in Figure 5.

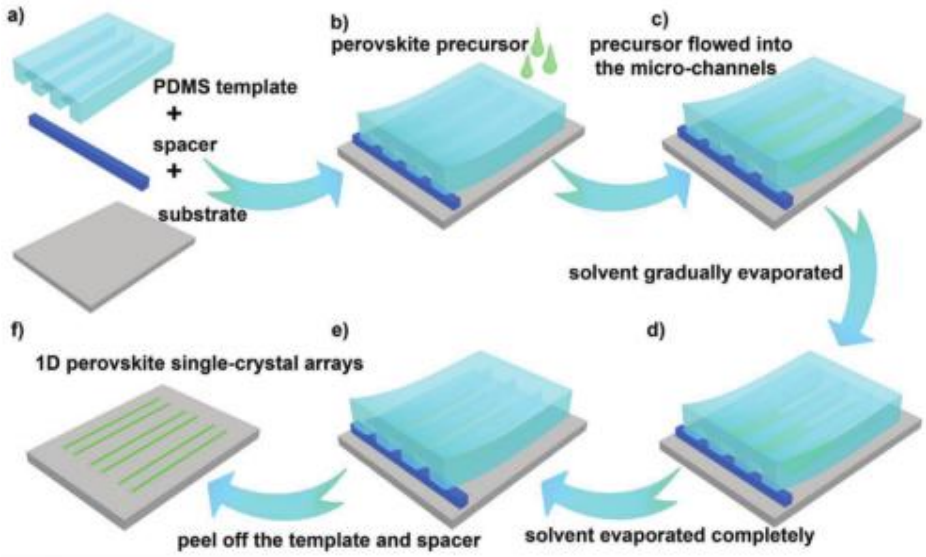

Figure 5. a) Microstructured PDMS film and spacer are tightly combined onto the substrate to form a series of periodically sealed microchannels. The spacer is used to support one end of the template to prevent the solvent evaporated from the PDMS template from being blown away from the substrate during the solvent evaporation process. b) $MAPbBr_3$ precursor is dropped onto one end of the template. c) Under the influence of capillary forces, the precursor quickly flows into these periodic microchannels. d) During the flow of the liquid through the channels, the solvent gradually evaporates, and two liquid tails attach to each side wall of the microchannels. Nucleation and crystallization occur along the channel sidewalls. e) After the evaporation of the solvent, $MAPbBr_3$ SCMWA remain on the substrate. f) After peeling off the PDMS template and spacer, highly aligned $MAPbBr_3$ SCMWA are obtained.

3. Low-Dimensional MHP PDs (Metal Halide Perovskite Photodetectors)

Semiconductor photodetectors are mainly classified into three types based on their structure: photodiodes, photoconductors, and phototransistors. The structures of various types of detectors are shown in Figure 6. [23] Photodiodes have a narrower charge transport distance and an internal electric field; therefore, they typically feature fast response speed, low noise, and high detection rate, but lower responsivity and external quantum efficiency (EQE). The working principle of a photodiode is as follows: when incident light with certain energy irradiates the junction, electrons transfer from the valence band to the conduction band, forming photogenerated electron-hole pairs. Under the influence of an electric field, minority carriers and photogenerated electron-holes in the depletion region move towards the electrodes at both ends, where they are collected, generating a photocurrent. In contrast, photoconductors, due to their photoconductive gain, have higher responsivity/EQE but generally exhibit slower response times and smaller detection rates. The working principle of a photoconductor is similar to that of a photodiode, except that the junction is usually a Schottky contact. Phototransistors will display balanced parameters between these three structures. For phototransistor detectors, due to their inherent amplification function, they typically show higher internal photocurrent gain.

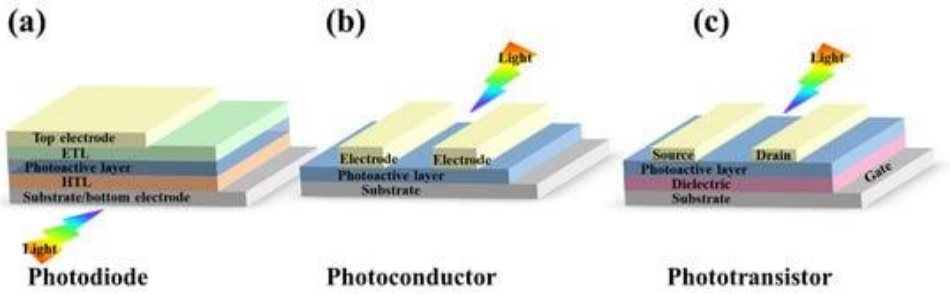

Figure 6. Schematic diagrams of different photodetector architectures. (a) Photodiode with a vertical structure. (b) Photoconductor with a lateral structure, and (c) Phototransistor with a bottom gate and top contact structure.

Low-dimensional halide perovskites refer to perovskite nanosheets (two-dimensional), nanowires (one-dimensional), or nanocrystals (zero-dimensional) where at least one dimension is on the nanoscale. They can also refer to certain perovskite materials that inherently possess a low-dimensional crystal structure (as shown in Figure 7).

Typically, the "low-dimensionality" of MHPs (Metal Halide Perovskites) is categorized into two types: "structural level" and "material level." "Structural level" low-dimensionality emphasizes the morphology of MHPs and usually refers to nanostructures, such as nanosheets, nanowires, and nanorods. In contrast, "material level" low-dimensionality focuses on the inherent crystal structure of MHPs, where [BX6]4− octahedra are separated by large dielectric spacer molecules, forming atomic-level 0D clusters, 1D quantum wires, or 2D quantum wells (QWs) in a block assembly. It is important to note that the zero-dimensional perovskite photodetectors reviewed in this chapter refer to perovskite materials that are zero-dimensional. However, since zero-dimensional materials cannot be directly used to fabricate photodetectors, they exhibit two-dimensional characteristics in their actual morphology.

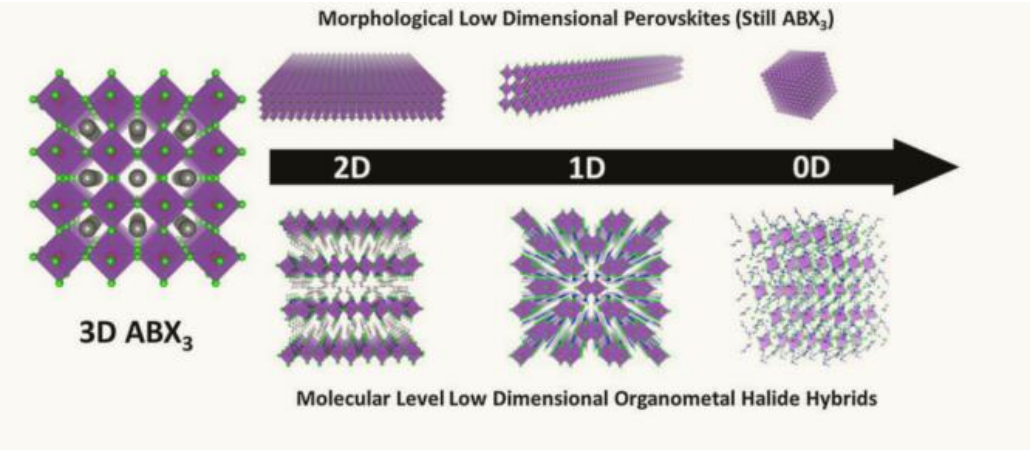

Figure 7. Three-dimensional ABX3 perovskites compared with halide perovskites possessing low-dimensional morphologies and crystal structures (Copyright 2018 Elsevier B.V. All rights reserved.)

3.1. PDs Based on 0D Perovskites

In recent years, hybrid perovskites have emerged as unique semiconductor materials for various optoelectronic device applications. Properties such as long carrier diffusion lengths, low exciton binding energy, easy bandgap tunability, and low-temperature solution processability make these materials highly useful in such devices. However, their poor stability under environmental conditions and the toxicity of lead hinders their commercial use.

The distinction between organic and inorganic perovskites primarily lies in the type of cation at the A-site. Organic perovskites have organic amines or other organic cations, such as $CH_3NH_3^+$ or $NH_2CH{=}NH_2^+$, at the A-site. Inorganic perovskites have inorganic metal or non-metal cations, like

Cs^+ or Bi_3^+, at the A-site. This difference affects the optoelectronic performance, stability, and toxicity of perovskites.

Generally, organic perovskites have higher photovoltaic conversion efficiency but are more prone to degradation due to humidity, temperature, and light exposure. [28] [29] [30]

The group led by Jakubas first reported $(CH_3NH_3)_3Bi_2I_9$ single crystals, composed of isolated double octahedra $[BiI_9]^{3-}$anions and nearly freely rotating $CH_3NH_3^+$ cations. However, their use of Weissenberg photographs only allowed them to suggest the space group P63/mmc. [24] In 1996, Kawai et al. synthesized $(CH_3NH_3)_3Bi_2I_9$ single crystals by mixing a certain amount of $(BiO_2)CO_3$ and CH_3NH_2 in a concentrated aqueous solution of HI and then cooling the saturated solution from 8°C to room temperature. At that time, the specific structure of this organic perovskite was unclear, preventing an understanding of its working mechanism and improvement of its optoelectronic properties. Thanks to Kaskel's research group, they were the first to clarify the correct crystal structure of 0D $(CH_3NH_3)_3Bi_2I_9$ perovskites. [25] $(CH_3NH_3)_3Bi_2I_9$ crystals belong to the hexagonal crystal system with the space group P63/mmc. In this structure, two Bi atoms located on different mirror planes bond with three equivalent symmetric bridging I_1 atoms and terminal I_2 atoms, forming $[Bi_2I_9]^{3-}$ complex anions, as shown in Figure 2c, with a slightly distorted octahedral coordination geometry. Thus, 0D (CH3NH3)3Bi2I9 comprises isolated coplanar $[Bi_2I_9]^{3-}$ clusters separated by methylammonium cations, with $[Bi_2I_9]^{3-}$ anions aligned along the c-axis. Once the structure of $(CH_3NH_3)_3Bi_2I_9$ was clearly understood, a surge of 0D $(CH_3NH_3)_3Bi_2I_9$ materials with excellent optoelectronic properties emerged through improved synthesis methods and material types.

Zheng et al. grew $MA_3Bi_2I_9$ perovskite single crystals using a seed crystal-assisted isothermal evaporation method. [26] They first heated a mixture of MAI and BiI_3 in α-butyrolactone (GBL) solution with a molar ratio of 3:2 at 6°C for 12 hours, filtering it with PTFE before use. Then, the precursor solution was maintained at 6°C for 24 hours to obtain $MA_3Bi_2I_9$ single crystal seeds, followed by adding one seed to fresh precursor solution at 7°C for 20 days. They finally obtained dark red-black $MA_3Bi_2I_9$ crystals, with sizes up to 27 mm. The prepared single crystals exhibited excellent thermal and environmental stability.

Furthermore, the organic cations in organic perovskites often contain lead, a heavy metal harmful to the environment and human health. Inorganic perovskites can use lead-free or low-lead alternatives, such as Sn_2^+ or Bi_3^+, thereby reducing their toxicity and environmental impact. Therefore, combining the advantages of both types of perovskite materials is a popular topic of current research. For example, Johnpaul K. Pious and colleagues prepared PDBI by treating lead iodide (PDI) and bismuth (III) iodide in aqueous hydroiodic acid solution at 9°C for 3 hours. [27] They filtered the solution under thermal conditions and dried the filtrate under vacuum to obtain a red powder-like crude product. Using methanol as a good solvent and chloroform as a poor solvent, they prepared a new type of lead-free, zero-dimensional organic perovskite material, $(PD)_2Bi_2I_{10}\cdot 2H_2O$ (PDBI, where PD is 1,3-propyldiammonium), using anti-solvent diffusion. Bismuth-based materials with ns2 electron configuration similar to Pb_2^+ were introduced into the perovskite structure, displaying improved electronic characteristics with a quantum well structure, without compromising the stability of the resulting discrete layers. Photodetectors made with PDBI showed a broad absorption spectrum in the visible light region from 350 to 600 nm (as shown in Figure 8), TGA indicated thermal stability up to 28°C, and the edge-sharing BiI_6^{3-} octahedra provided rigidity to the perovskite framework, in turn offering better moisture resistance. Most importantly, it displayed consistent and reproducible photocurrents over several light on/off cycles.

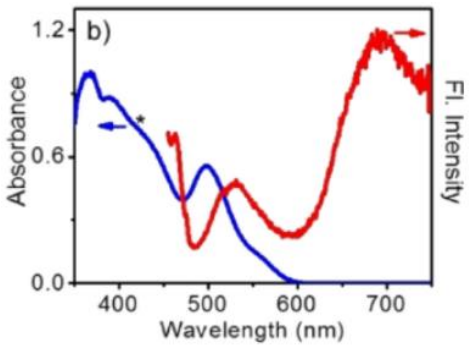

Figure 8. PDBI exhibits a broad absorption spectrum in the visible light region from 350 to 600 nm.

The on/off ratio of the PDBI photodetector, calculated from the light (194 nA) and dark currents (94 nA), is 2.1. This ratio is comparable to that reported for one-dimensional perovskites like $(C_6H_{13}N)_2BiI_5$ (on/off ratio = 2.9) and (N, N, N', N'-tetramethylpiperidine) $1.5[Bi_2I_7Cl_2]$ (on/off ratio = 3). The device's responsivity is measured at 1.14 mA/W. Besides responsivity, other important advantages of the photodetector device include the specific detectivity and the number of electrons detected per incident photon (external quantum efficiency, EQE). For PDBI, these parameters are estimated to be 1.9×10^6 Jones and 0.4%, respectively. More importantly, the photocurrent is consistent and reproducible over several light on/off cycles. The aforementioned properties of PDBI, along with comparisons to other lead-free zero-dimensional perovskites, indicate that the former is an excellent candidate for optoelectronic device applications.

Inorganic perovskites exhibit better stability and durability, but are also more challenging to achieve efficient charge transport and separation.

Tang and colleagues reported a photodetector made using a 0D non-toxic single-crystal perovskite, Cs_3BiBr_6, deposited on ITO electrodes. [31] This photodetector showed an increase in photocurrent with increasing light intensity and voltage (Figure 9a), and the device was able to respond to periodic light ON and OFF cycles, producing stable photocurrent signals repeatedly (Figure 9b). Additionally, the material achieved an ultra-low dark current of 0.3 nA under a 6V bias and a high detectivity of 0.8×10^9 Jones at room temperature, demonstrating its potential in photodetector applications. Furthermore, 0D Cs_3BiBr_6 exhibited high stability against temperature and humidity, which contributes to enhancing the stability of photodetectors.

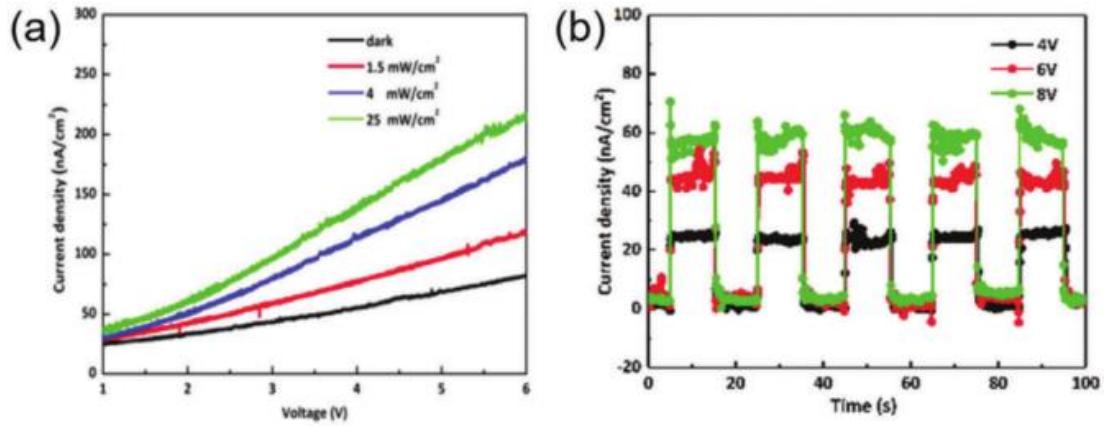

Figure 9. a) I–Vcharacteristics of0D Cs_3BiBr_6-based photodetector under the dark and light illumination with different light densities. b) Photocurrent responses under various bias voltages with fixed light density of 25 mW cm^{-2}. a, b) Reproduced with permission.[122] Copyright 2019, The Royal Societyof Chemistry.

Subsequently, by altering the metal halides used in the deposition process, Xie et al. [32] synthesized another type of 0D lead-free perovskite, $Rb_7Bi_3Cl_{16}$, with a cluster structure. This perovskite is composed of two types of octahedra with different octahedral distortions (Δd), namely,

discrete $[BiCl_6]^{3-}$ octahedra and $[Bi_2Cl_{10}]^{4-}$ edge-sharing dimers, with Rb+ cations filling the spaces (Figure 10). The $[BiCl_6]^{3-}$ octahedra, located on the surface of the crystal cell, have no distortion ($\Delta d1 = 0$). The $[Bi_2Cl_{10}]^{4-}$ dimers, located internally, have a larger distortion ($\Delta d2 = 0.84$). The increased presence of surface $[BiCl_6]^{3-}$ octahedra in $Rb_7Bi_3Cl_{16}$ contributes to its enhanced moisture stability.

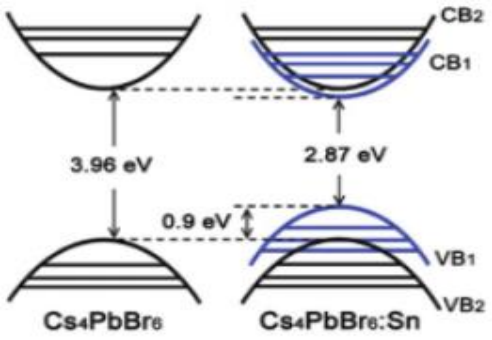

Figure 10. Octahedra with different Δd values.

In addition to the deposition method, highly stable 0D inorganic perovskite materials can also be synthesized through a simple hydrothermal method. For example, Gong and colleagues synthesized 0D $Cs_3Sn_3F_2Cl_7$ single crystals using this hydrothermal method. [33] They dissolved CsF and $SnCl_2 \cdot H_2O$ in a mixture of H_2O, sealed it in an autoclave lined with Teflon, and heated it at 22℃ for one day. It was then slowly cooled to room temperature at a rate of 3 Ch^{-1} per hour. Finally, by washing the reaction product with deionized water and ethanol, colorless and transparent crystals were obtained. Using the same method, Xie and team synthesized 0D $Rb_7Bi_3Cl_{16}$ single crystals by dissolving RbCl and $BiCl_3$ in a mixture of HCl in a stainless-steel autoclave lined with PTFE and heating it at 16℃ for 24 hours. The mixture was then slowly cooled to room temperature at a rate of 2 Ch^{-1} per hour and washed with water.

Although the work of Tang, Xie, and Gong has produced perovskite materials meeting the requirements for high stability in photodetectors, the pure phase of uniform 0D Cs_4PbBr_6 NC has not yet been reported. This is mainly due to the uncontrolled nucleation rate in those conventional methods. There is an urgent need for a novel synthesis approach. Zhang et al. designed a reverse-phase microemulsion method to synthesize Cs_4PbBr_6 nanoparticles with a uniform size distribution of about 26 nm. [34] Our method overcomes the issue of impurity phases and, by carefully choosing reactants and stoichiometric ratios, leads to selectively produced 0D rhombohedral phase Cs_4PbBr_6 NCs with an 85% reaction yield. The photoluminescence quantum yield (PLQY) of the colloidal solution form is 65%. Notably, it can be drop-casted to produce thin films with a high PLQY of 54%. Reverse-phase emulsion synthesis can be easily scaled up for kilogram-level production. For example, in a single scale-up experiment, 0.2 g of Cs_4PbBr_6 NC was synthesized in a 100 mL solution. The crystal structure of Cs_4PbBr_6 makes their NCs resistant to anionic exchange because the cage-like $PbBr_6^{4-}$ octahedra are inaccessible, which is distinctly different from the behavior of other perovskite NCs. Our work opens up many possibilities for the design and practical use of perovskite crystals with new 0D phases.

3.2. PDs Based on 1D Perovskites

Single-crystal halide perovskite nanowires (NWs) have attracted widespread attention for their use in high-performance photodetectors (PDs) due to their high photoluminescence quantum yields, large carrier mobility, and long carrier diffusion lengths. Compared to PC perovskite thin films, single-crystal perovskite NWs with defined structures can provide more direct paths for charge transport, resulting in higher photoluminescence (PL) quantum yields, greater carrier mobility, and longer carrier diffusion lengths [49-51]. The advantages of perovskite NWs suggest that PDs using these NWs should exhibit high performance. Additionally, the anisotropic geometric structure of one-

dimensional perovskites enables PDs based on one-dimensional perovskites to have special potential applications in linear dichroic photodetection.

Semiconductor single crystals, with higher phase purity, fewer grain boundaries, and defects, are more suitable for fundamental and applied research in optoelectronics than polycrystalline and amorphous materials due to their ability to enhance the device's figure of merit. Li et al. successfully grew high-quality, well-defined, millimeter-sized $CsCu_2I_3$ single crystals using a low-cost solution processing method. [37] They fabricated a broadband photodetector based on one-dimensional all-inorganic $CsCu_2I_3$ single crystals with high stability and fast response. This device exhibited stable broadband (300-700 nm) UV-visible light responses, including responsivities of 10.0-52.0 mA W^{-1}, specific detectivity of (1.8-9.3) × 10^{10} Jones, EQE of 2.3-19% (at 3V bias), and fast response times (rise time = 0.19 ms, decay time = 14.7 ms at 350 nm and 10 V bias), outperforming most reported all-inorganic lead-free metal halide-based photodetectors. (as shown in Figure 11)

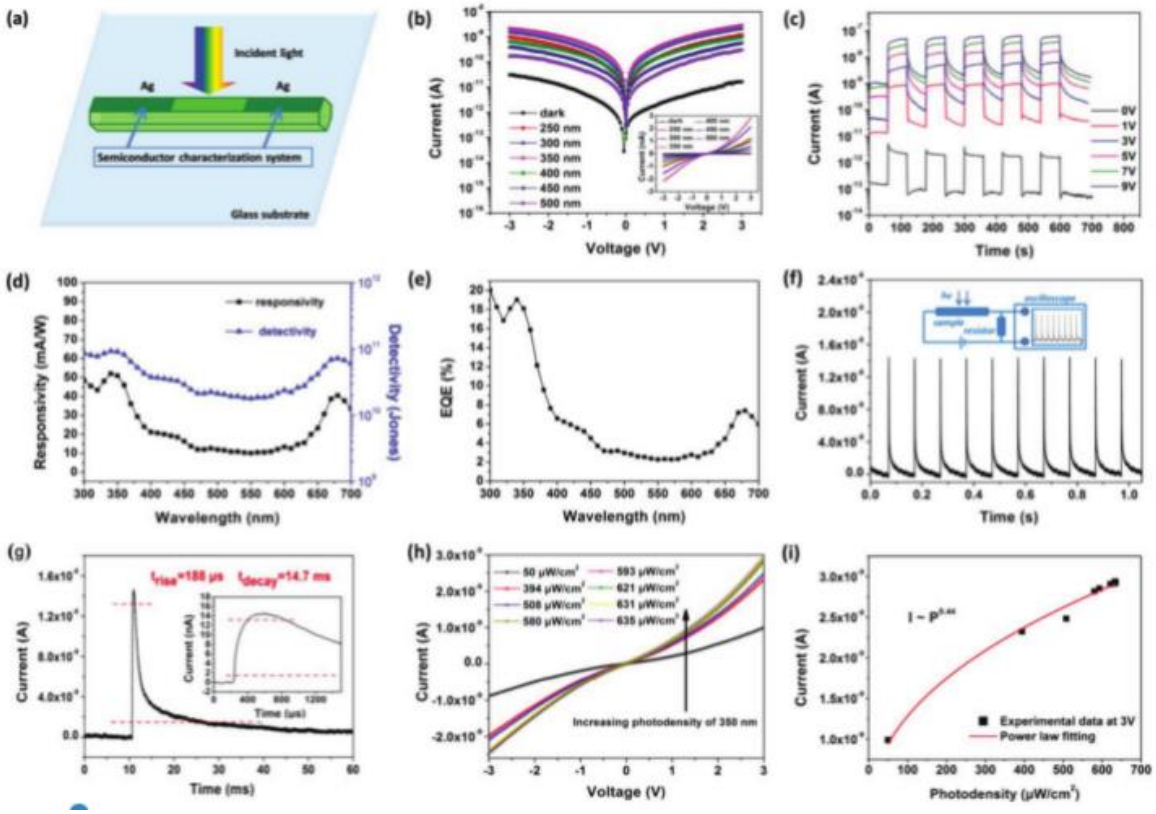

Figure 11. Photodetector performance of $CsCu_2I_3$ on the (010) plane: a) Schematic illustration of the $CsCu_2I_3$ photodetector. b) I-V curves under dark and 250-500 nm illumination. c) I-t curves under 350 nm irradiation at 0-9V bias. d) Responsivity and detectivity curves calculated at 3V bias for 300-700 nm. e) EQE curves calculated at 3V for 300-700 nm. f) Photoresponse to 10 Hz 355 nm laser pulses at 10V bias. g) Rise and decay times estimated from single-pulse response curve; inset shows the magnified curve. h) Light intensity-dependent I-V curves under 350 nm irradiation. i) Photocurrent as a function of light intensity and corresponding power law fitting curves under 350 nm irradiation at 3V bias.

Due to the rapid degradation of halide perovskites in the presence of oxygen and moisture, integrating perovskite photodetectors onto low-temperature flexible substrates to improve the physical stability of perovskite-based devices has become a current research focus. One-dimensional perovskite materials, with their high controllability and fabricability in the one-dimensional direction, are easy to integrate, making them ideal candidates for fabricating such devices. Y M. Asuo used a low-temperature two-step spin-coating method to deposit a network of $CH_3NH_3PbI_3$ nanowires and a protective PMMA film onto a Kapton substrate, creating a broadband flexible photodetector. [38] Figure 13a illustrates the fabrication process of the perovskite nanowires. Initially, a PbI_2: Pb (SCN_2

layer was directly spin-coated onto a Kapton film substrate. Subsequently, a methylammonium iodide precursor solution in isopropanol: N, N-dimethylformamide was deposited on top of the PbI_2: Pb (SCN_2 layer. The film was then annealed on a hot plate at 11℃ at room temperature to remove solvents and generate a network of perovskite nanowires before depositing the gold electrodes. Finally, a protective PMMA film was deposited onto the perovskite layer by spin-coating, with the final device configuration shown in Figure 13b. The device demonstrated high photo response and a high specific detectivity of 7.3×10^{12} Jones, along with response times of 227.2 μs (rise) and 215.4 μs (decay). The thin PMMA layer passivates and protects the perovskite nanowires from moisture, thereby enhancing the device's performance and stability (the encapsulated device retained more than 98% of its initial photocurrent after 30 days of storage in ambient air).

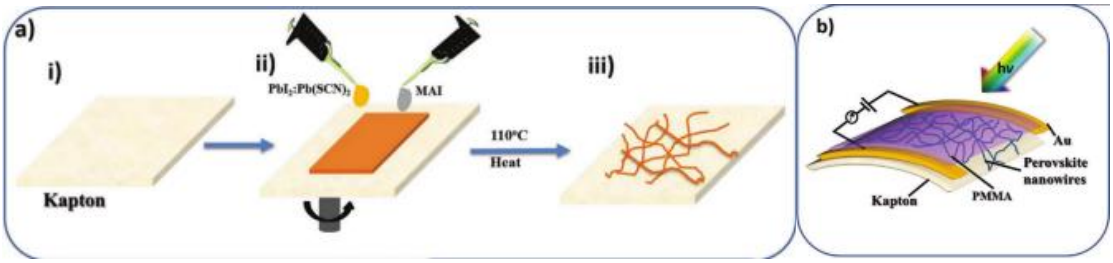

Figure 12. a) Schematic illustration (i-iii) of synthesizing and depositing a perovskite nanowire network on a flexible Kapton substrate using the spin-coating method. b) Device configuration of the flexible perovskite photodetector.

Li et al. employed a template-assisted method to fabricate methylammonium lead bromide ($MAPbBr_3$) micro/nanowire structures [39]. The combination of a protective layer, high crystalline quality, and highly ordered microstructure enabled the $MAPbBr_3$ single-crystal microfiber arrays to retain 96% of their initial photocurrent after one year without further encapsulation. The lifespan of this photodetector is about four times longer than that of the most stable perovskite micro/nanocrystal-based photodetectors previously reported; it is considered the most stable perovskite photodetector reported to date!

So far, most high-performance NW PDs have been manufactured based on single or aligned NWs requiring complex fabrication processes. Deng et al. [40] reported a Fluid-Guided Anti-solvent Vapor-Assisted Crystallization (FGAVC) method for mass manufacturing of oriented single-crystal $MAPb(I_{1-x}Br_x)_3$ NW arrays. PDs made from these NW arrays exhibited high performance, with a responsivity (R) of 12500 $A \cdot W^{-1}$ and a Linear Dynamic Range (LDR) of 115 dB.

This approach for high-performance perovskite NW PDs requires complex fabrication processes and faces the challenge of producing high-performance self-powered PDs. To achieve self-powered characteristics, p-n junctions or Schottky barriers are needed. However, the difficulty of p- or n-type doping in perovskites [42] and complex nanoscale manipulation [43-48] pose significant obstacles for single or aligned perovskite NW PDs. Photodetectors with a p-i-n vertical structure, where the perovskite NW network is sandwiched between an electron-selective layer (ESL) and a hole-selective layer (HSL), are a promising option. Zhou et al. reported a self-powered perovskite $CsPbBr_3$ NW PD with a vertical p-i-n structure [41], where $CsPbBr_3$ NWs were prepared by a combination of solution-phase processes and halide exchange (SPP-HE). This CsPbBr3 NW PD not only achieved ultra-low dark currents and high photocurrent densities but also had a responsivity of up to 0.3 $A \cdot W^{-1}$, specific detectivity of 1.0×10^{13} Jones, an on/off ratio of 10^6, a linear dynamic range (LDR) of 135 dB, and excellent self-powered performance.

However, self-powered photodetectors with a vertical p-i-n structure can suffer from loss of incident light and the accumulation of interface defects. To address these issues, Wang et al. successfully fabricated a photodetector based on lateral $CsPbI_3$-$CsPbBr_3$ heterojunction nanowire arrays using an in-situ conversion and electrode fabrication method (as shown in Figure 13) [49]. This device reduces the direct light contact of the active layer, thus minimizing light reflection and loss, and the small contact area of the heterojunction can decrease defects. It boasts an impressive

responsivity of 125 mA·W^{-1} at zero bias, along with fast rise and decay times of 0.7 and 0.8 ms, respectively.

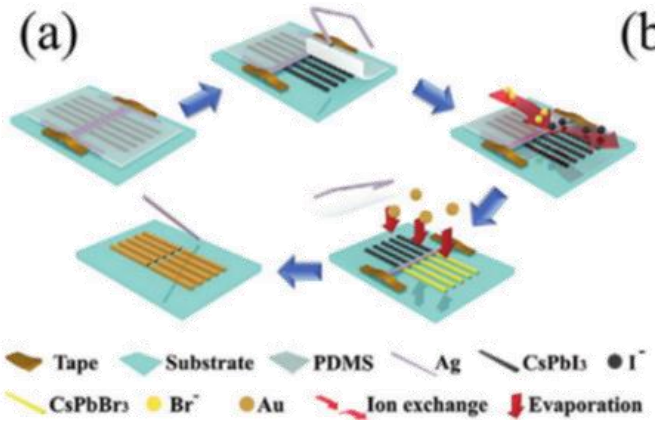

Figure 13. Schematic illustration of the main fabrication process for a self-powered photodetector.

In recent years, ultrabroadband photodetectors (UB-PDs) capable of detecting a wide spectrum (ultraviolet-visible-infrared-terahertz) have gradually become a hot topic in international research. Most photodetectors are responsive only to ultraviolet-visible light associated with their bandgap (around 2.3 eV). Cao et al. integrated $CsPbBr_3$ nanowire arrays with near-infrared (NIR) sensitizing materials to create a high-performance self-powered photodetector capable of ultraviolet-visible-near-infrared (UV-vis-NIR) detection. [50] This hybrid device exhibits a wide response spectrum from 300 to 950 nm, high responsivity of 0.25 A·W^{-1}, a large detectivity of 1.2×10^{13} Jones, and fast response speeds of up to 111/306 μs.

The relatively high dark current still limits the further development of perovskite photodetectors. Reduced dark current is a key feature for high-performance photodetectors. Gui et al. adopted a simple, low-cost two-step solution processing method at room temperature to prepare all-inorganic $CsPbBr_3$ microfibers with a surface rich in nanocrystals. [51] Assembled on indium tin oxide (ITO) electrodes, the optimized photodetectors based on these $CsPbBr_3$ polycrystalline single micro-wires exhibited considerably low dark current and noise, leading to an improved detectivity of $>10^{12}$ Jones. Moreover, these devices did not compromise other performances: they also showed a high responsivity of up to 118 A·W^{-1} and fast response within 40 ms, making the $CsPbBr_3$ micro-wire photodetectors suitable for miniaturized, high-detectivity, and rapid-response applications.

Most fabricated perovskite nanowires underperform due to poor crystalline quality and rough surfaces. Additionally, precise alignment and patterning of perovskite nanowires are necessary for large-scale integrated devices. Deng et al. used a simple Fluid-Guided Anti-solvent Vapor-Assisted Crystallization (FGAVC) method, which slows down the crystallization process and provides a moisture-isolated growth environment, to obtain perovskite nanowires with smooth surfaces. [52] This device achieved a photodetector responsivity of up to 12,500 A·W^{-1} and a wide linear dynamic range (LDR) of 150 dB, the best values ever reported for perovskite-based photodetectors!

The unique geometric shape of one-dimensional perovskites enables special applications in linear dichroic photodetection for photodetectors based on one-dimensional perovskites. Gao et al. synthesized $CH_3NH_3PbI_3$ nanowire arrays using a one-step self-assembly method with oleic acid (OA) soaking passivation. [53] This device exploited the anisotropic geometric structure of $CH_3NH_3PbI_3$ nanowires to achieve strong polarization-dependent light detection in a perovskite photodetector for the first time. It exhibited sub-millisecond response times, a responsivity of 4.95 A·W^{-1}, and a measured detectivity of 2×10^{13} Jones. This is the highest detectivity reported to date for any $CH_3NH_3PbI_3$-based photodetector, further expanding the potential applications of organic-inorganic hybrid perovskite photodetectors.

Table 1. Summarizes all the performance parameters of the photodetectors discussed in this section for comparison.

Material	CsCu2I3 Single Crystal Nanowires	CH3NH3PbI3 Nanowire	Self-Powered CsPbBr3 Nan	MAPb(I-xBrx	UV-vis-NIR Self-Powered	Lateral CsPbI3-CsP	CsPbBr3 Polycrost	MAPbBr3 Single Crys	CH3NH3PbI3 Nanowir
Responsivity /A*W^{-1}	0.01-0.052	0.62	0.3	12500	0.25	0.125	118	20	4.95
On/Off Ratio			10^6						
EQE	2.3%-19%						10^4%		
Detectivity /Jones	1.8×10^{10}~9.3×10^{10}	7.3×10^{12}	1.0×10^{13}		1.2×10^{13}	1×10^{12}		4.1×10^{12}	2×10^{13}
LDR/dB			135	115					
Spectral Selectivity /nm	300-700				300-950		350-?		
Response Time τ_{rise}/τ_{decay}	0.19ms/14.7ms	227μs/15 μs			111μs/306 μs	0.7ms/0.8 ms	38ms/36 ms		Sub-millisecond

3.3. PDs Based on 2D Perovskites

Broadly, two-dimensional perovskite materials do not merely refer to their two-dimensional geometric structure. Due to the unique composition of their material structure, electrons or holes are confined by quantum size effects to move freely only in two dimensions (usually in planes perpendicular to the film growth direction) over a nanoscale range (1-100nm), while their movement is restricted in the third dimension (usually the direction of film growth), forming quantum wells that limit electron motion. In a narrower sense, two-dimensional perovskite materials refer to perovskites with a two-dimensional crystal structure, such as large planes and thin thicknesses, like micro or nanosheets or micro or nanodisks. By controlling reaction conditions and limiting the growth rate of different crystal planes, oriented growth of perovskite on different crystal planes can be achieved, thereby controlling the thickness and producing numerous small-sized two-dimensional perovskite materials.

Over the past two years, various synthesis techniques like chemical vapor deposition, one-step solution self-assembly, and colloidal chemistry have led to the development of two-dimensional nanostructures of ABX_3 type halide perovskites, such as microdisks (MD), nanoplatelets (NPLs), and nanosheets (NS). [54] These nanostructured perovskites have naturally formed multiple quanta well structures, layered structures, and tunable bandgaps, exhibiting high PL quantum yield, quantum confinement and size effects, long electron diffusion lengths, and increased exciton binding energy, making them promising for different optoelectronic device applications. Recent studies have focused on material synthesis, device structural design, interface engineering, and physical mechanism analysis to improve device characteristics, including stability, sensitivity, response speed, and device noise.

Although perovskite-based photodetectors have also seen widespread development with excellent performance, unfortunately, two-dimensional perovskite photodetectors, limited by an intrinsic bandgap of ≈1.5 eV, mainly operate in the visible spectrum, making them challenging candidates for infrared communication detection applications. However, Zhang et al. successfully deposited $CH_3NH_3PbI_3$ perovskite films onto erbium yttrium silicate (EYS) nanoplates, creating a novel perovskite-EYS nanoplate hybrid waveguide photodetector. [55] This perovskite-EYS nanoplate composite photodetector exhibited a sub-bandgap photoresponsivity of ≈0.11 $mA\cdot W^{-1}$, an average Quantum Efficiency (EQE) of 0.01%, and a response time of 900 μs. Compared to previous sub-bandgap photodetectors, it maintained a comparable responsivity and EQE while offering a faster response time.

Recent research has made significant advancements in improving the photoelectric performance and stability of two-dimensional perovskites through material and structural design.

Wang and colleagues developed a high-performance flexible photodetector based on $(BA)_2FAPb_2I_7$ perovskite by optimizing film quality and device structure. [56] This detector exhibited rapid response and excellent environmental stability. The film's quality and crystallinity were enhanced by adding FACl as an additive. Furthermore, the performance was further improved by

embedding Au nanostructures into the substrate to introduce localized surface plasmon resonance, enhancing the interaction between light and matter. The optimized device achieved a response speed of 9μs and maintained good long-term environmental stability (>1000 hours), with a maximum responsivity of 2.3 $A \cdot W^{-1}$ and detectivity of 3.2×10^{12} Jones.

Shan et al. developed an ultrafast responsive and high detectivity self-powered photodetector based on $MAPbI_3$ perovskite films, using a star-shaped small molecule with a triazine core, Triazine-Th-OMeTAD, as a dopant-free hole transport layer. [57] The optimized Triazine-Th-OMeTAD perovskite photodetector exhibited a low dark current of 1.09 nA/cm^2 at zero bias, high responsivity of 0.47$A \cdot W^{-1}$, and a detectivity exceeding 8.2×10^{12} Jones, along with a rapid response speed of 18 ns.

Cai et al. prepared high-quality two-dimensional perovskite $(PEA)_2PbI_4$ films (as shown in Figure 14) using a solution method at a low annealing temperature (80°C) without any special treatments and further fabricated a photodetector. [58] The results showed that this photodetector had a low dark current (10^{-11} A), good responsivity (107 $mA \cdot W^{-1}$) at 450 nm illumination, and a high detectivity (2.05×10^{12} Jones). The most challenging aspect of this work was to improve the quality of the two-dimensional perovskite films while reducing fabrication costs and simplifying the production process.

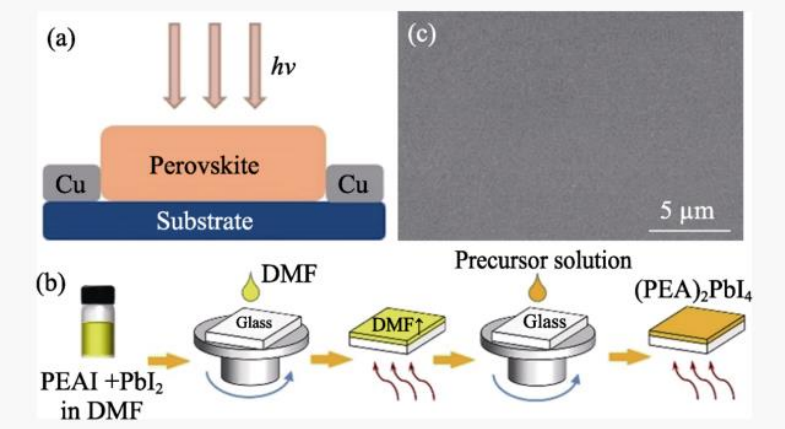

Figure 14. (a) Device structure of the photodetector prepared on a glass substrate, (b) Schematic diagram of the $(PEA)_2Pb_{14}$ film preparation process, and (c) SEM image of the $(PEA)_2Pb_4$ film after annealing at 8°C.

Although photodiodes based on polycrystalline films can suppress dark currents, they cannot achieve significant photoconductive gain, resulting in less-than-ideal device sensitivity. Feng et al. prepared $(BA)_2(MA)_{n-1}PbnI_{3n+1}$ (where BA = butylammonium, MA = methylammonium, and n = layer number, 2–5 in this study) by controlling the crystal growth of two-dimensional perovskites through asymmetric interfacial wetting. [59] Electron diffraction and synchrotron grazing-incidence X-ray scattering revealed that the prepared nanowires exhibited single orientation, with conductive few-layer perovskites and butylammonium ion layer assembly forming a superlattice structure. Fluorescence and photoconductivity measurements on nanowires of different heights showed that the perovskite layer's edges effectively split excitons, generating and conducting free charge carriers, resulting in excellent photoconductivity. Photodetectors prepared based on these nanowires achieved responsivity of over 10^4 $A \cdot W^{-1}$ and a detectivity exceeding 7×10^{15} Jones, surpassing the performance of traditional silicon photodiodes by 2-3 orders of magnitude. It is currently the most sensitive perovskite photodetector in the world!

Table 2. Summarizes all performance parameters of the photodetectors in this section for comparison.

Material	Responsivity /A*	Switchin	EQE	Detectivity/Jones	LDR/dB	Spectral Selectivity	Response Time
CH 3 NH3 PbI 3-EYS Nanocomposite	0.11×10^{-3}		0.01%			Near-Infrared	900µs /900µs
(BA) 2 (MA)Pb2I7 Single Crystal		10^3	200%	10^{11}	89		
Optimized (BA) 2FAPb2I7 Perovskite Film	2.3			3.2×10^{12}			9µs/ 9µs
MAPbI3 Perovskite Film	0.47			8.2×10^{12}			18 ns/ 18 ns
(PEA) 2 PbI 4 Perovskite Film	0.107			2.05×10^{12}			
Optimized (BA) 2 (MA)n−1PbnI3n+1 two-dimensional perovskite	104			7×10^5			

4. Conclusions and Outlook

This article reviews recent progress in perovskite-structured photodetectors, focusing on the dimensions of the perovskite structure (including 0D quantum dots, 1D nanowires and microwires, and 2D nanostructures), synthesis and modification methods, composition, photodetection performance, and applications. There exists some controversy in the academic community regarding photodetectors based on low-dimensional perovskites. Some researchers view them as promising and valuable for future applications, while others question their performance and practical applicability. These controversies are primarily centered around material performance, device fabrication, and application performance. Further research and analysis of these academic disputes, offering reasonable explanations and insights, will help better understand and grasp the limitations and breakthroughs in the study of low-dimensional perovskite photodetectors.

Regarding 0D perovskite photodetectors, their instability still restricts their practical applications. These stability issues include the instability of 0D perovskite materials under conditions of oxygen, moisture, heat, and light exposure; powder quenching; and color segregation in mixed compositions. To address the instability issues of 0D perovskites, they are often stabilized by long-chain organic ligands, such as oleic acid. 0D perovskite materials with these ligands demonstrate good stability in both solutions and films.

Photodetectors based on 1D nanowires and microwires show improved performance due to their low defect/trap density, long charge carrier lifetimes, and reduced carrier recombination rates. However, their random and rough morphology still poses challenges in using 1D perovskites for photodetection applications, and these issues need to be addressed to achieve better performance. Traditional lithographic techniques can damage the perovskite crystal structure, so suitable processes for fabricating perovskite micro-nano arrays must be developed. For perovskite materials with low solubility, liquid-phase methods are ineffective, thus necessitating the development of a new, universal, simple, and efficient method for preparing perovskite microcrystal arrays.

The challenges with 2D perovskites mainly focus on scalability issues, making it difficult to achieve uniformity in large-area manufacturing, and pose challenges in device integration. To address manufacturing issues, vacuum thermal evaporation under vacuum conditions allows for good film thickness uniformity, high-quality film formation, and process stability, making it suitable for large-scale production. For integration challenges, adjusting the cations acting as spacers and the asymmetric lattice structure for optical cavity engineering may enable breakthroughs in the integration of 2D perovskite materials in nonlinear optical devices.

References

[1] A Review of Perovskite-Based Photodetectors and Their Applications by Haiyan Wang, Yu Sun College of Sciences, Shanghai Institute of Technology, 100 Haiquan Road, Shanghai 201418, China Authors to whom correspondence should be addressed.

[2] Perovskite photodetectors and their application in artificial photonic synapses Xin Huang,Yunlong Guo.

[3] High-Performance Photodetectors Based on Nanostructured Perovskites by Chunlong Li.

[4] Metal Halide Perovskite Nanowires: Controllable Synthesis, Mechanism, and Application in Optoelectronic Devices by Yangbin Lu.

[5] Liu Jia, et al. Preparation and Performance Regulation of Two-Dimensional Perovskite/Graphene Heterojunction Photodetectors [J]. Science China Chemistry, 2022, 52 (2): 11 - 20.

[6] PbI2-DMSO Assisted in Situ Growth of Perovskite Wafers for Sensitive Direct X-Ray Detection Wenjun Liu.

[7] ZHANG Yafei, et al. Low Temperature Growth of Single Crystals of Tin-Lead Mixed Perovskite and Its Application in Chiral Light Detection [J]. China Science Daily, 2022, 67 (10): 1023 - 1030.

[8] Self-Driven Perovskite Narrowband Photodetectors with Tunable Spectral Responses Jian Wang, Shuang Xiao, Wei Qian, Kai Zhang, Jun Yu, Xiuwen Xu, Gaopeng Wang, Shizhao Zheng, and Shihe Yang* Adv. Mater. 2020, 2005557, DOI: 10.1002/adma. 202005557.

[9] Inch-sized high-quality perovskite single crystals by suppressing phase segregation for light-powered integrated circuits.

[10] PbI_2-DMSO Assisted In-situ Growth of Perovskite Wafer for Sensitive Direct X-ray Detector.

[11] A.K. Jena, A. Kulkarni, T. Miyasaka, Halide perovskite photovoltaics:

[12] Nonlinear Photonics Using Low-Dimensional Metal-Halide Perovskites: Recent Advances and Future Challenges Weiqiang Chen.

[13] Low-Dimensional Metal Halide Perovskite Photodetectors Hsin-Ping Wang, Siyuan Li, Xinya Liu, Zhifeng Shi, Xiaosheng Fang, * and Jr-Hau He* background, status, and future prospects. Chem. Rev. 119, 3036 – 3103 (2019).

[14] Multidimensional $CsPbX_3$ Inorganic Perovskite Materials: Synthesis and Solar Cells Application Ying Yang.

[15] Y.-C. Hsiao et al., Fundamental physics behind high-efficiency organo-metal halide perovskite solar cells. J. Mater. Chem. A 3, 15372 – 15385 (2015).

[16] Herz L M. Charge-carrier mobilities in metal halide perovskites: fundamental mechanisms and limits [J]. ACS Energy Letters, 2017, 2 (7): 1539 - 1548.

[17] Research progress of low-dimensional perovskite photodetectors.

[18] Aligned Single-Crystalline Perovskite Microwire Arrays for High-Performance Flexible Image Sensors with Long-Term.

[19] Ultrahigh-Responsivity Photodetectors from Perovskite Nanowire Arrays for Sequentially Tunable Spectral Measurement.

[20] Scalable All-Evaporation Fabrication of Efficient Light-Emitting Diodes with Hybrid 2D – 3D Perovskite Nanostructures.

[21] Large-Area Perovskite Nanowire Arrays Fabricated by Large-Scale Roll-to-Roll Micro-gravure Printing and Doctor Blading.

[22] Perovskite single-crystal microwire-array photodetectors with performance stability beyond 1 year.

[23] Lead-Free Halide Double Perovskite for High-Performance Photodetectors: Progress and Perspective by Xiaoyan Li.

[24] a) R. Jakubas, J. Zaleski, L. Sobczyk, Ferroelectrics 1990, 108, 109; b) R. Jakubas, L. Sobczyk, Phase Transitions 1990, 20, 163.

[25] K. Eckhardt, V. Bon, J. Getzschmann, J. Grothe, F. M. Wisser, S. Kaskel, Chem. Commun. 2016, 52, 3058.

[26] X. Zheng, W. Zhao, P. Wang, H. Tan, M. I. Saidaminov, S. Tie, L. Chen, Y. Peng, J. Long, W.-H. Zhang, J. Energy Chem. 2020, 49, 299.

[27] Zero-Dimensional Lead-Free Hybrid Perovskite-like Material with a Quantum-Well Structure

[28] Zhou, C., Lin, H., Tian, Y. et al. Luminescent zero-dimensional organic metal halide hybrids with near-unity quantum efficiency. Chem. Sci. 9, 586 – 593 (2018).

[29] Zhang, X., Lin, H., Huang, H. et al. Lead-Free, Air-Stable All-Inorganic Cesium Bismuth Halide Perovskite Nanocrystals. Angew. Chem. Int. Ed. 56, 12471 – 12475 (2017).

[30] Zhou, C., Lin, H., Shi, Z. et al. Lead-Free, Zero-Dimensional Hybrid Perovskites with Broadband and Ultrabright Photoluminescence. ACS Energy Lett. 3, 54 – 61 (2018).

[31] Y. Tang, M. Liang, B. Chang, H. Sun, K. Zheng, T. Pullerits, Q. Chi, J. Mater. Chem. C 2019, 7, 3369.

[32] J.-L. Xie, Z.-Q. Huang, B. Wang, W.-J. Chen, W.-X. Lu, X. Liu, J.-L. Song, Nanoscale 2019, 11, 6719.

[33] P. Gong, S. Luo, K. Xiao, Q. Huang, Y. Yang, H. Huang, Y. Wu, C. Chen, Z. Lin, Inorg. Chem. 2017, 56, 3081.

[34] Zero-Dimensional Cs_4PbBr_6 Perovskite Nanocrystals.

[35] Y. Xu, B. Jiao, T.-B. Song, C. C. Stoumpos, Y. He, I. Hadar, W. Lin, W.Jie, M. G. Kanatzidis, ACS Photonics 2019, 6, 196.

[36] X. Zheng, W. Zhao, P. Wang, H. Tan, M. I. Saidaminov, S. Tie, L. Chen, Y. Peng, J. Long, W.-H. Zhang, J. Energy Chem. 2020, 49, 299.

[37] Facet-Dependent, Fast Response, and Broadband Photodetector Based on Highly Stable All-Inorganic $CsCu_2I_3$ Single Crystal with 1D Electronic Structure Ziqing Li, Ziliang Li, Zhifeng Shi, * and Xiaosheng Fang*.

[38] Highly Efficient and Ultrasensitive Large-Area Flexible Photodetector Based on Perovskite Nanowires y M. Asuo, Paul Fourmont, Ibrahima Ka, Dawit Gedamu, Soraya Bouzidi, Alain Pignolet, Riad Nechache, * and Sylvain G. Cloutier*.

[39] Perovskite Single-Crystal Microwire-Array Photodetectors with Performance Stability beyond 1 Year Shun-Xin Li, Yi-Shi Xu, Cheng-Long Li, Qi Guo, Gong Wang, Hong Xia, * Hong-Hua Fang,Liang Shen,* and Hong-Bo Sun*.

[40] W. Deng, L. Huang, X. Xu, X. Zhang, X. Jin, S.T. Lee, J. Jie, Nano Lett. 17 (4) (2017) 2482–2489.

[41] Self-powered $CsPbBr_3$ nanowire photodetector with a vertical structure Hai Zhou, Zhaoning Songb, Corey R. Griceb, Cong Chenb, Jun Zhanga, Yifan Zhua, Ronghuan Liua, Hao Wanga, ∗, Yanfa Yanb, ∗.

[42] Q. Ou, Y. Zhang, Z. Wang, J.A. Yuwono, R. Wang, Z. Dai, W. Li, C. Zheng, Z.Q. Xu, X. Qi, S. Duhm, Adv. Mater. 30 (2018) 1705792.

[43] M. Spina, E. Bonvin, A. Sienkiewicz, B. Náfrádi, L. Forró, E. Horváth, Sci. Rep. 6 (2016) 19834.

[44] W. Deng, L. Huang, X. Xu, X. Zhang, X. Jin, S.T. Lee, J. Jie, Nano Lett. 17 (4) (2017) 2482–2489.

[45] L. Gao, K. Zeng, J. Guo, C. Ge, J. Du, Y. Zhao, C. Chen, H. Deng, Y. He, H. Song, G. Niu, Nano Lett. 16 (12) (2016) 7446 – 7454.

[46] W. Deng, X. Zhang, L. Huang, X. Xu, L. Wang, J. Wang, Q. Shang, S.T. Lee, J. Jie, Adv. Mater. 28 (11) (2016) 2201 – 2208.

[47] T. Yang, Y. Zheng, Z. Du, W. Liu, Z. Yang, F. Gao, L. Wang, K.C. Chou, X. Hou, W. Yang, ACS Nano 12 (2018) 1611 – 1617.

[48] P. Gui, Z. Chen, B. Li, F. Yao, X. Zheng, Q. Lin, G. Fang, ACS Photonics (2018), https: //doi.org/10.1021/acsphotonics. 7b01567.

[49] Flexible and Self-Powered Lateral Photodetector Based on Inorganic Perovskite $CsPbI_3$–$CsPbBr_3$ Heterojunction Nanowire Array Meng Wang, Wei Tian, Fengren Cao, Min Wang, and Liang Li*.

[50] Self-Powered UV–Vis–NIR Photodetector Based on Conjugated-Polymer/$CsPbBr_3$ Nanowire Array Fengren Cao, Wei Tian, Kaimo Deng, Meng Wang, and Liang Li*.

[51] High-performance photodetectors based on single all-inorganic $CsPbBr_3$ perovskite microwire Pengbin Gui, Zhao Chen, Borui Li, Fang Yao, Xiaolu Zheng, Qianqian Lin, and Guojia Fang.

[52] Ultrahigh-Responsivity Photodetectors from Perovskite Nanowire Arrays for Sequentially Tunable Spectral Measurement Wei Deng, Liming Huang, Xiuzhen Xu, Xiujuan Zhang, Xiangcheng Jin, Shuit-Tong Lee, and Jiansheng Jie*.

[53] Passivated Single-crystalline $CH_3NH_3PbI_3$ Nanowire Photodetector with High Detectivity and Polarization Sensitivity Liang Gao, Kai Zeng, Jingshu Guo, Cong Ge, Jing Du, Yang Zhao, Chao Chen, Hui Deng, Yisu He, Haisheng Song, Guangda Niu, and Jiang Tang.

[54] Two-Dimensional Materials for Halide Perovskite-Based Optoelectronic Devices Shan Chen and Gaoquan Shi*.

[55] Perovskite–Erbium Silicate Nanosheet Hybrid Waveguide Photodetectors at the Near-Infrared Telecommunication Band Xuehong Zhang, Shuzhen Yang, Hong Zhou, Junwu Liang, Huawei Liu, Hui Xia, Xiaoli Zhu, Ying Jiang, Qinglin Zhang, Wei Hu, Xiujuan Zhuang, Hongjun Liu,Weida Hu, Xiao Wang, and Anlian Pan*.

[56] High performance and Stable Plasmonic-FunctionalizedFormamidinium-Based Quasi-2D Perovskite Photodetector forPotential Application in Optical Communication Tao Wang, Daming Zheng, Jike Zhang. Jie Qiao, Changjun Min, Xiaocong Yuan, Michael SomekhFu Feng.

[57] An ultrafast-response and high-detectivity self-powered perovskite photodetector based on a triazine-derived star-shaped small molecule as a dopant-free hole transporting layer Chengwei Shan, ‡a Fei Meng,‡a Jiahao Yu, a Zhangxia Wang,c Wenhui Li, a Dongyu Fan,a Rui Chen, a Haibo Ma, c Gongqiang Li *b and Aung Ko Ko Kyaw.

[58] Photodetector Based on Two-dimensional Perovskite $(PEA)_2PbI_{4\ CAI}$ Kai, JIN Zhiwen.

[59] Single-crystalline layered metal-halide perovskite nanowires for ultrasensitive photodetectors. Jiangang Feng,Cheng Gong,Hanfei Gao,Wen Wen,Yanjun Gong,Xiangyu Jiang,Bo Zhang,Yuchen Wu,Yishi Wu,Hongbing Fu, Lei Jiang & Xiang Zhang.

[60] Physics of high-performance photodetectors and devices based on perovskite materials Huang.

[61] Self-trapped state enabled filterless narrowband photodetections in 2D layered perovskite single crystals Junze Li, Jun Wang, Jiaqi Ma, Hongzhi Shen1, LuLi, Xiangfeng Duan & Dehui Li.